

Article

Possibility of Advanced Modified-Silica-Based Porous Materials Utilisation in Water Adsorption Processes—A Comparative Study

Karol Sztekler ^{1,*}, Agata Mlonka-Mędrala ¹, Nezar H. Khdary ², Wojciech Kalawa ¹, Wojciech Nowak ¹ and Łukasz Mika ¹

¹ Faculty of Energy and Fuels, AGH University of Science and Technology, Mickiewiczza 30, 30-059 Krakow, Poland; amlonka@agh.edu.pl (A.M.-M.); kalawa@agh.edu.pl (W.K.); wnowak@agh.edu.pl (W.N.); lmika@agh.edu.pl (Ł.M.)

² King Abdulaziz City for Science and Technology, Riyadh 11442, Saudi Arabia; nkhdary@kacst.edu.sa

* Correspondence: sztekler@agh.edu.pl

Abstract: Due to a high risk of power outages, a heat-driven adsorption chillers are gaining the attention. To increase the efficiency of the chiller, new adsorbents must be produced and examined. In this study, four newly developed silica-based porous materials were tested and compared with silica gel, an adsorber commonly paired with water. Extended sorption tests using mercury intrusion porosimetry, gas adsorption, and dynamic vapor sorption were performed. The morphology of the samples was determined using a scanning electron microscope. The thermal properties were defined using simultaneous thermal analysis and a laser flash method. Metal organic silica (MOS) nanocomposites analysed in this study had thermal properties similar to those of commonly used silica gel. MOS samples have a thermal diffusivity coefficient in the range of 0.17–0.25 mm²/s, whereas silica gel of about 0.2 mm²/s. The highest water adsorption capacity was measured for AFSMo-Cu and equal to 33–35%. For narrow porous silica gel mass uptake was equal about 25%. In the case of water adsorption, it was observed that the pore size of the sorbent is essential, and adsorbents with pore sizes higher than 5 nm, are most recommended in working pairs with water.

Keywords: metal organic silica; nanocomposites; sorption; thermal diffusivity; adsorption chiller



Citation: Sztekler, K.; Mlonka-Mędrala, A.; Khdary, N.H.; Kalawa, W.; Nowak, W.; Mika, Ł. Possibility of Advanced Modified-Silica-Based Porous Materials Utilisation in Water Adsorption Processes—A Comparative Study. *Energies* **2022**, *15*, 368. <https://doi.org/10.3390/en15010368>

Academic Editors: Adrián Mota Babiloni and Laura Savoldi

Received: 22 October 2021

Accepted: 29 December 2021

Published: 5 January 2022

Publisher's Note: MDPI stays neutral with regard to jurisdictional claims in published maps and institutional affiliations.



Copyright: © 2022 by the authors. Licensee MDPI, Basel, Switzerland. This article is an open access article distributed under the terms and conditions of the Creative Commons Attribution (CC BY) license (<https://creativecommons.org/licenses/by/4.0/>).

1. Introduction

Adsorption chillers are cooling devices that use heat instead of electricity. The main advantages of this type of chillers are quiet and easy operation, high reliability, and the absence of moving mechanical parts (except valves), as well as the possibility of water desalination [1]. However, their disadvantages include: a relatively low coefficient of cooling performance COP, usually in the range of 0.5 to 0.6, low specific cooling power SCP, small mass and heat transfer in the adsorption bed, as well as considerable dimensions and large weight [2]. To increase the competitiveness of adsorption chillers in the cooling devices market, the performance parameters must be constantly improved. Companies manufacturing sorption cooling devices are looking for more advanced adsorbate-adsorbent working pairs and construction materials.

In this study, a group of new advanced materials is considered as effective adsorbents in adsorption chillers that work in pairs with water. Nanocomposites were synthesised through incorporation of metal nanoparticles into silica matrix.

Metal-organic silica (MOS) are dynamically developing materials with significant industrial potential, because of the wide range of useful properties such as high stability and resistibility to chemical changes [3]. The mesoporous structure of the silica matrix and extensive surface area of about 1500 m²/g [4] enables to obtain material with high sorption capacity [5,6]. Modification of MOS properties is performed through introduction

of additional atoms or functional groups [4,7]. The unique features of MOS make them candidates for a variety of applications such as wastewater treatment [8], CO₂ sequestration [9], catalysis [10,11], as heavy metal adsorbents [12,13] and other toxic contaminants detectors and adsorbents [14,15].

Metal-doped mesoporous silica obtained by spray drying was examined by Endo et al. to enhance its water adsorption capacity [16]. Very promising results were obtained also by Yanagihara et al. who was testing Zr-doped two-dimensional hexagonal mesoporous silica (Zr-MPS) in working pair with water, in this case a water uptake of about 70 g/g was noted [17].

Water used as an adsorbate in this study, is a readily available, cheap and nontoxic adsorbate, which is additionally characterised by high environmental friendliness. Another benefit is the possibility of desalination of water from seas and oceans in adsorption chiller and increase of global drinking water resources [18–20]. Moreover, water is the most thermally stable adsorbate, and its heat of vaporization is higher than in the case of other refrigerants [21]. However, since its evaporation in the evaporator takes place in a low pressure environment (below atmospheric pressure), it is necessary to create a vacuum inside the system, which will reduce the reliability of the entire device due to the additional risk of leakage. In combination with an extremely tight structure, it allows to eliminate the possibility of air leakage, which could result in incorrect adsorption, evaporation or condensation. Furthermore, water has a very low saturation pressure compared to the other types of adsorbates [22].

In this study, four novel adsorbents and one reference material were analysed in a working-pair with water. The presented results cover a knowledge gap regarding the possibilities and limitations of sorbents utilization in water vapour adsorption processes, with a special input on adsorption cooling devices. A minimal pore size diameter was determined for sorbents used in working pair with water. To properly address the problem of adsorbents used in sorption cooling devices, sorption properties and structure were examined, as well as thermal properties of all analysed materials were also tested.

2. Materials and Methods

The present study is a comparative analysis of new adsorbents of high potential to be used in adsorption chillers. In addition to water uptake capacity, thermal properties and morphology were examined to make a proper comparison of the materials.

2.1. Materials

Three samples of metal-organic silica (MOS) nanomaterials, and a sample of highly porous silica sorbent were delivered by a research group from King Abdulaziz City for Science and Technology. In this study also a commercial sample of silica gel was tested as a reference material. Narrow porous silica gel, of particle size 2–7 mm was manufactured by Chemland. The photographs of the analysed sorbents are presented in Figure 1.

The samples analysed in the study were as follows:

- Metal Organic Silica: AFSPd-Cu in the form and colour similar to the fine sand, AFSPd-Cu (NP) (MOS with metal nanoparticles (NP)) material was similar to the previous one, but the colour of the sample was grey, AFSMo-Cu in the form of small blue crystals,
- High-porous silica material MPSilica: which was a very fine white powder.
- Narrow porous silica gel of particle size 2–7 mm.

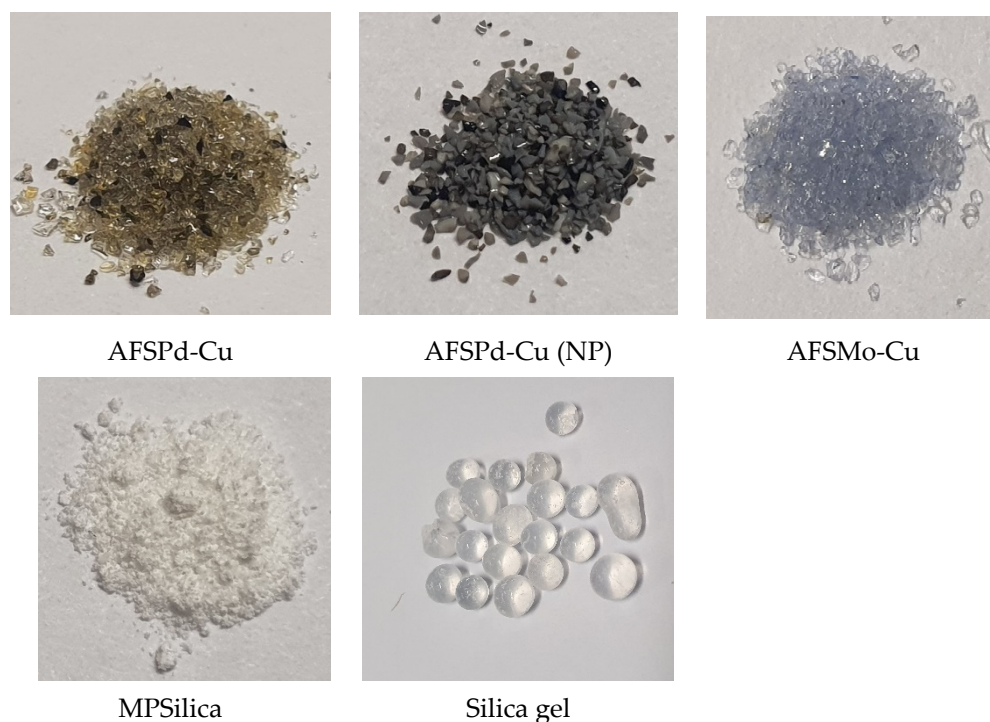


Figure 1. Photographs of the samples analysed in the study.

2.2. Methods

Several analytical methods were used to determine sample morphology and structure, together with thermal and sorption properties. The STA method was used to analyse thermal decomposition of the materials in an adsorption chiller working temperature range. The experiments were carried out on a Mettler Toledo high-temperature thermogravimetric analyser. The sorbents were placed in aluminium oxide crucibles, the temperature range was from the ambient temperature to 300 °C at a constant heating rate of 10 °C/min in 50 mL/min air. TG, DSC, and DTG curves were prepared.

The morphology of the sorbents was analysed using a scanning electron microscope coupled with energy-dispersive X-ray (Nova NanoSEM 450) to identify the chemical composition of the materials. In this study, the morphology was tested at a beam acceleration voltage of 2 kV, whereas EDS tests were performed at 15 kV up to 30 kV.

Structural analyses of the materials were performed using two methods. First, the analysis was performed on an ASAP 2020 volumetric analyzer (Micromeritics) using low-pressure nitrogen physisorption at -196 °C. The specific surface area and average pore diameter of each sample were determined using the Brunauer–Emmet–Teller (BET) model based on the adsorption isotherms with P/P_0 ranging between 0.06 and 0.20. The total volume of the pores was determined by applying the Brunauer–Emmet–Teller (BET) and Barrett–Joyner–Halenda (BJH) methods to the adsorption and desorption curves. Average pore diameters were calculated on the basis of total pore volume and surface area.

Mercury intrusion porosimetry was used to determine the effective porosity, as it does not include closed porosity, which is inaccessible to the injected mercury. The method shows pore size distributions of mesopores and macropores. Quantachrome Poremaster 33 was used to define the pore size distribution in the range of ~ 7 nm to 1 mm.

The Laser Flash Method was used to analyse thermal properties of the sorbents in this work. The method allows to determine the thermal diffusivity coefficient of the given solid material. In this study, samples were tested using Netzsch LFA 457 MicroFlash. In this apparatus, the thermal diffusivity coefficient is defined automatically with a measurement accuracy equal to $\pm 3\%$. The measurement conditions of thermal diffusivity were performed with argon flow rate of 50 mL/min at four temperatures: 30, 40, 50, and 60 °C. Before the measurement all samples were grounded into dust.

Water sorption properties of samples examined in this study were determined using Dynamic Gravimetric Vapor Sorption System DVS Vacuum. The sample mass during the adsorption and desorption processes is constantly measured by the equipment, the measurement is characterised by high sensitivity, equal to 0.1 μg . The stability of the temperature at 25 $^{\circ}\text{C}$ is equal to ± 0.02 $^{\circ}\text{C}$ and the humidity conditions generated are typically in the range of $\pm 0.1\%$ with respect to the given value [2]. In this study, water was used as an adsorbate. Before the experiment, approximately 20 mg of sample was dried, the sample was placed in the apparatus at 100 $^{\circ}\text{C}$ for 60 min. After 60 min of stabilisation at a given process temperature, a series of 20 experimental stages of 20 min, each started. Each stage had a different setting of a relative pressure P/P_0 , starting from 10% to 100%. On the basis of experimental results, adsorption and desorption isotherms were calculated. The water intake for all samples was obtained depending on its saturation pressure. The steam flow rate was set constant and equal to 15 sccm (standard cubic centimeters per minute). The experiment was carried out at four process temperatures: 30, 40, 50, and 60 $^{\circ}\text{C}$.

3. Results and Discussion

The results of the performed experiments are presented and discussed in detail in this Section. Adsorbents were compared according to their thermal and sorption properties. An additional comparison was performed with previously published studies.

3.1. Structural Analysis and Morphology

Figure 2 shows SEM images of the sorbents analysed, the structure and morphology of the sorbents are an essential factor revealing how developed is the porous structure of the materials. More SEM images were included in Supplementary Materials in Figures S1–S5.

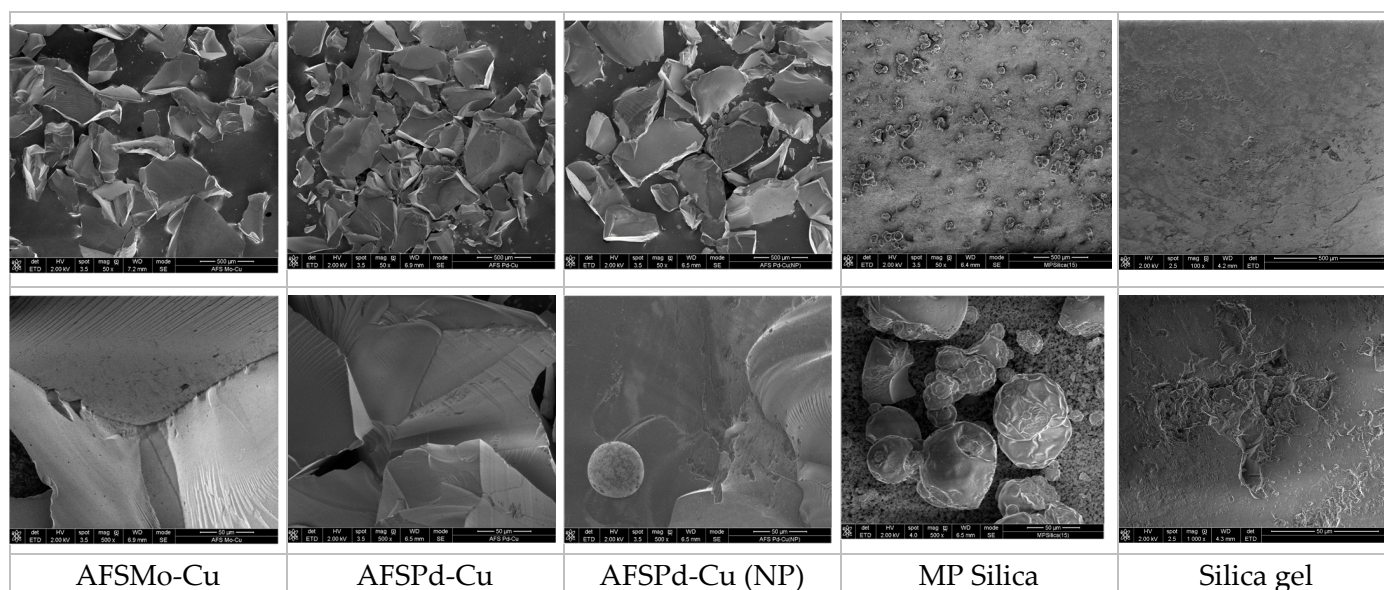


Figure 2. Morphology analysis of adsorbents analysed in this study.

MOS samples denoted as AFS group had a very similar morphology. They consist of irregular particles of various shapes and sizes. The structure of the sorbent particles was smooth and sharp. The average size of these particles was approximately 500 μm . In some images, areas where “grooves” appear on the surface or a “stepped” structure are present. Fine round pores on the surface of the particles might be observed at some points. In the case of samples doped with metal nanoparticles—AFSPd-Cu (NP), also sphere-shaped metal particles were present.

The MPSilica sorbent was a heterogeneous material. The particle size was not uniform, but most particles were characterised by an irregular spherical shape. In this sample, there

are present large particles (up to approx. 80 μm), these particles had a developed surface, and smaller particles stuck or grown on them to form agglomerates. In addition, this sorbent consisted of a large number of very fine round particles, approx. 1 μm in size, which also formed agglomerates. These very small particles also stuck to larger particles. The pores were not visible in the photographs, what might be associated with the microporous structure of the material.

Silica gel is characterised by a very uniform structure, regular shape of the sorbent is recommended for sorption chiller adsorption bed. Small damages in adsorbent structure showed internal, porous morphology of the material.

EDS analysis was used to determine the chemical composition, but the results of the analysis are not clear because the peaks from some elements were poorly visible. Table 1 summarises the selected results of the quantitative EDS analysis for individual samples. The main constituent of all tested sorbents was SiO_2 with some additives which are determined in the samples names. It should be noted that the amounts of doped elements are rather small.

Table 1. Chemical composition of the analysed sorbents on the basis of EDS analysis, wt.%.

Sample	C	O	Si	F	S	Cl	Ni	Mo	Cu	Pd	Na
MP Silica (15)	-	49.2	50.8	-	-	-	-	-	-	-	-
AFS Mo-Cu	-	54.6	42.9	-	-	-	-	1.4	1.2	-	-
AFS Pd-Cu	-	56.3	40.6	-	-	1.0	-	-	0.6	1.5	-
AFS Pd-Cu (NP)	-	51.7	42.3	-	-	-	-	-	0.5	3.5	2.0
Silica gel	8.6	49	42.4	-	-	-	-	-	-	-	-

3.2. Porosity

In this study, two different metal-organic silica nanoparticles with high potential for water adsorption were selected, one of them, AFSMo-Cu, had a moderate BET surface area, not exceeding 300 m^2/g , while the AFSPd-Cu sample had a specific surface area greater than 600 m^2/g . Both samples differed in mean pore diameters, in the case of nanocomposite with molybdenum addition, the mean pore diameter was about 5 nm, whereas in the case of the Pd-doped sample, this value was two times lower. The addition of metal nanoparticles to the AFSPd-Cu sample significantly reduced the specific surface area of the material, over 10 times, and an increase in the mean pore diameter was observed, which also increased almost 10 times.

In general, metal-organic silica nanocomposites are characterised by noticeable active surface area, exceeding in some cases 1000 m^2/g [23], but in the literature MOS with lower BET surface area were also reported [3]. However, it was noted that for porous materials with developed surface area like e.g.: MOFs, a BET surface area exceeding 7000 m^2/g is an indicator of the potential for the use of sorbents in adsorption chillers [24].

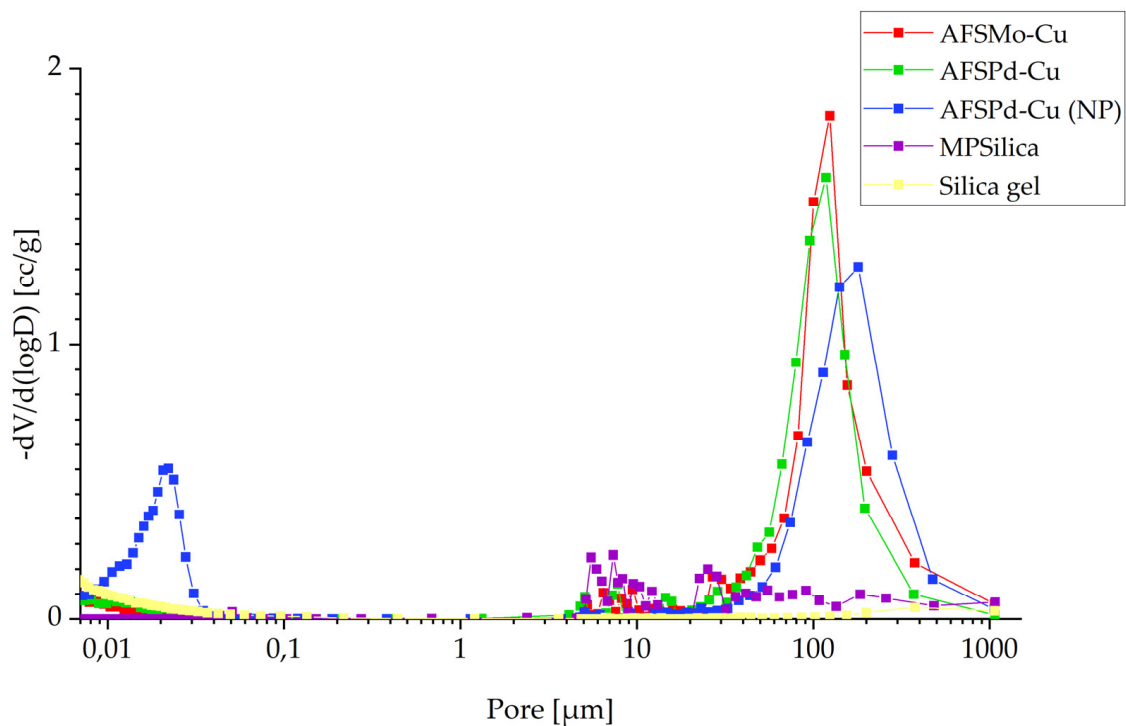
The material with the highest BET specific surface area was a highly porous silica-based material, MPSilica with a BET specific surface area exceeding 2000 m^2/g , this material was also characterised by narrow pores with a diameter of about 2.5 nm.

The analysis of summation curves as well as the pore size distribution during adsorption and desorption processes shows that, in most cases, a very wide unimodal pore distribution is observed. Table 2 summarizing the results of the gas sorption analysis shows the average values and the average values for a given maximum.

Mercury intrusion porosimetry is a technique frequently used to determine the volume of macropores and the size distribution of pores in adsorbents [25,26]. The results of mercury intrusion porosimetry—pore distribution and cumulative pore volume—are shown in Figures 3 and 4, respectively.

Table 2. Summary of BET + BJH analysis results.

Sample	BET Surface Area, m ² /g	Micropore Volume, m ³ /g	External Surface Area, m ² /g	Adsorption Average Pore Diameter (4 V/A by BET), nm	Desorption Average Pore Diameter (4 V/A by BET), nm	BJH Adsorption Average Pore Diameter (4 V/A), nm	BJH Desorption Average Pore Diameter (4 V/A), nm
AFSMo-Cu	283.71	21.08	262.63	5.21	5.21	4.87	3.95
AFSPd-Cu	636.62	42.11	594.51	2.50	2.50	3.29	2.84
AFSPd-Cu (NP)	51.86	4.67	47.19	21.59	21.14	23.22	15.12
MPSilica	2144.68	0	3956.55	2.64	2.61	3.02	2.62
Silica gel	789.18	204.29	584.89	2.19	2.19	3.24	2.75

**Figure 3.** Pore distribution determined using mercury intrusion porosimetry.

The distribution of the pores in Figure 3 shows that for MOS materials, the highest recorded initial increase related to the presence of macropores was observed. For the range of pore diameter between 100 and 200 μm , the highest values of the total pore volume were observed, which will be influenced both by the fact that they are the pores with the largest volume, but in this case their number could also be significant. For MPSilica, the highest number of pores was in the size of 5 to 20 μm . The cumulative pore volume in Figure 4 was associated with the pore distribution and sorbents characterised by a smaller pore size had a noticeably smaller pore volume.

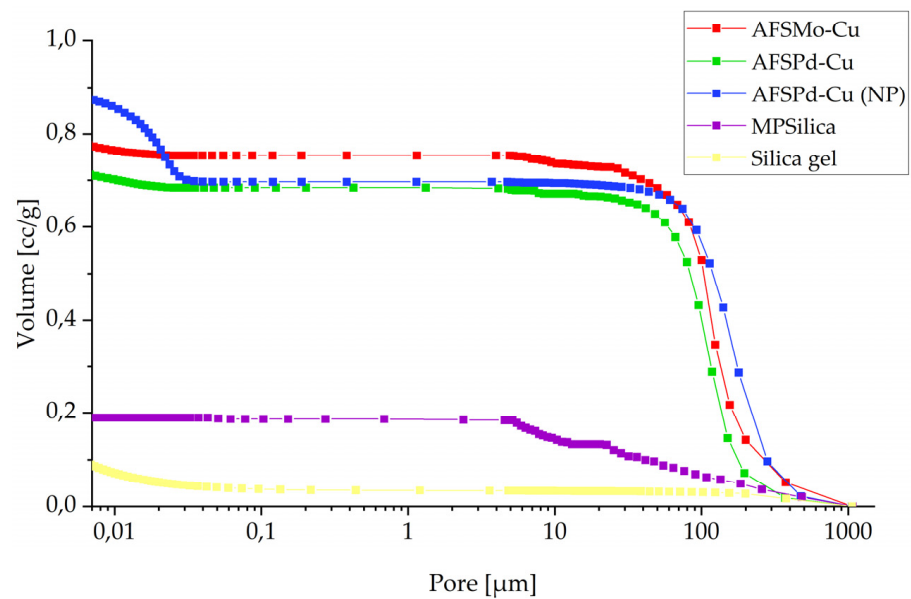


Figure 4. Cumulative pore volume determined using mercury intrusion porosimetry.

3.3. Thermal Diffusivity Coefficient

The results of thermal diffusivity coefficient, together with a measurement uncertainty equal to the standard deviation, are shown in Figure 5.

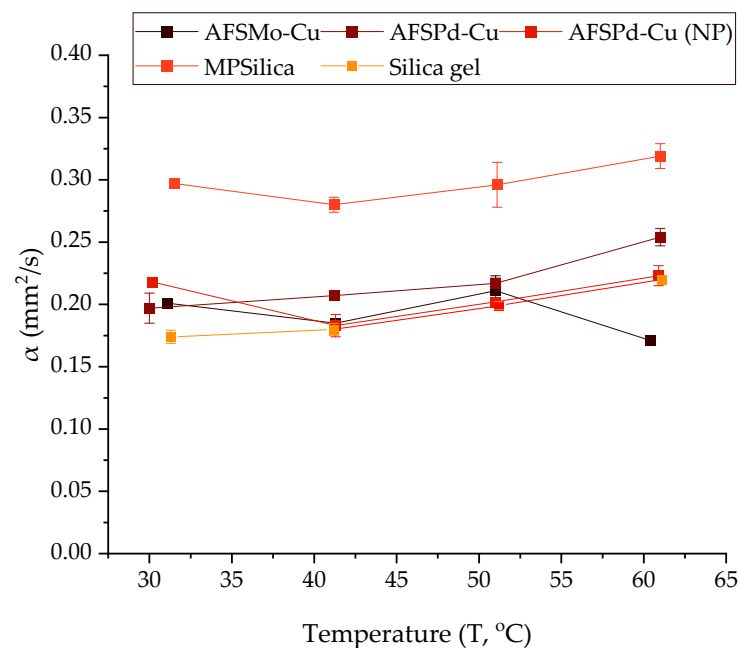


Figure 5. Thermal diffusivity coefficient of selected samples measured at four process temperatures (30, 40, 50, 60 °C).

The highest thermal diffusivity coefficient was measured for the MPSilica sample—about $0.3 \text{ mm}^2/\text{s}$, while the lowest was measured for silica gel—about $0.2 \text{ mm}^2/\text{s}$ for both samples. The interesting thing is that the tested sorbents were characterised by a stable value of the thermal diffusivity coefficient. In the analysed temperature range the thermal diffusivity coefficient in all cases was constant or slightly increased with temperature. Compared to the most commonly used adsorbent in sorption cooling devices, silica gel, whose thermal diffusivity is $0.137 \text{ mm}^2/\text{s}$ [20], thermophysical properties of the analysed sorbents are slightly higher.

3.4. Sorption Characteristics

The water intake was tested in the temperature range of 30–60 °C, the sorption isotherms are shown in Figures 6–10.

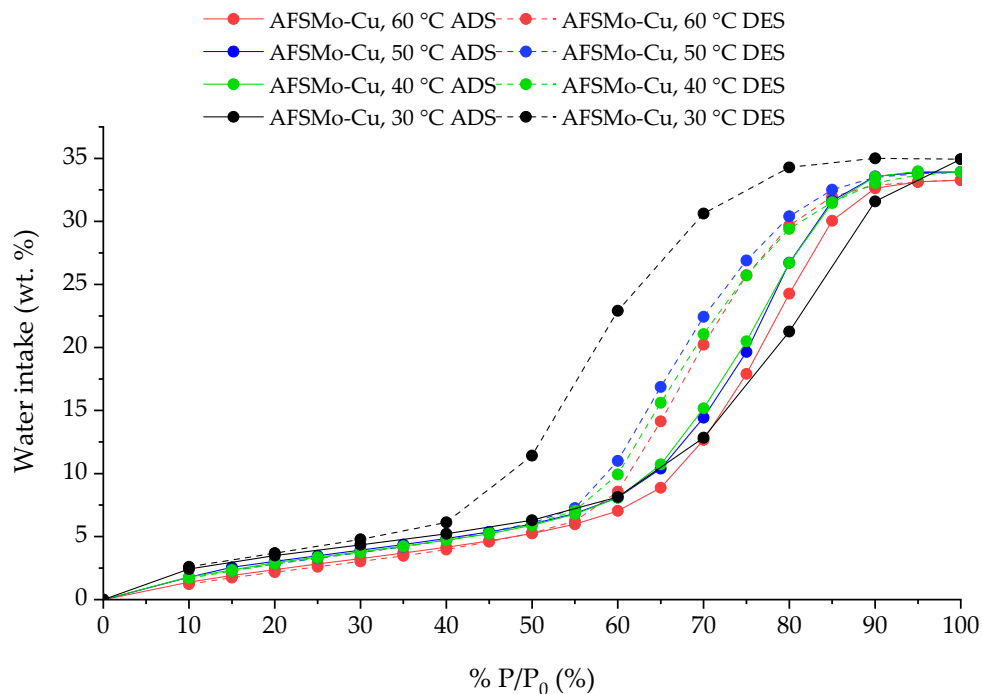


Figure 6. Adsorption and desorption isotherms for the AFSMo-Cu sample, at 30, 40, 50, and 60 °C.

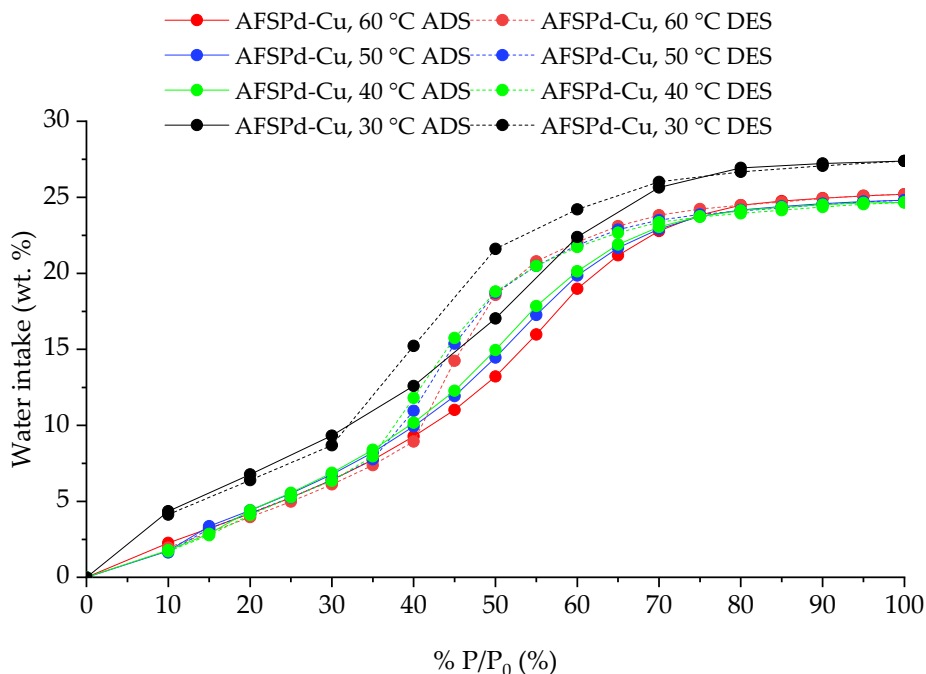


Figure 7. Adsorption and desorption isotherms for the AFSPd-Cu sample, at 30, 40, 50, and 60 °C.

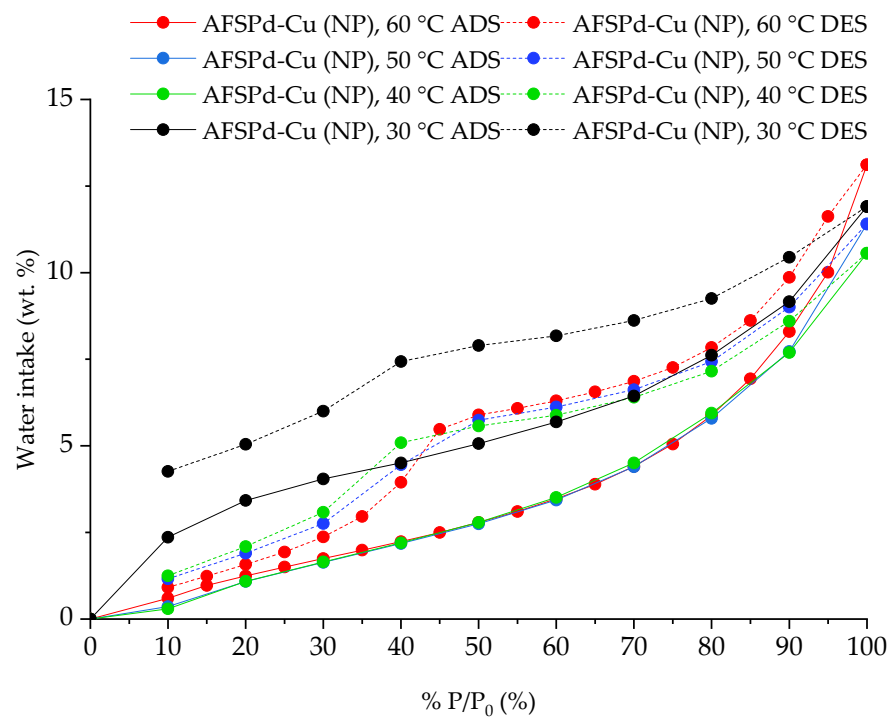


Figure 8. Adsorption and desorption isotherms for AFSPd-Cu (NP) sample, at 30, 40, 50 and 60 °C.

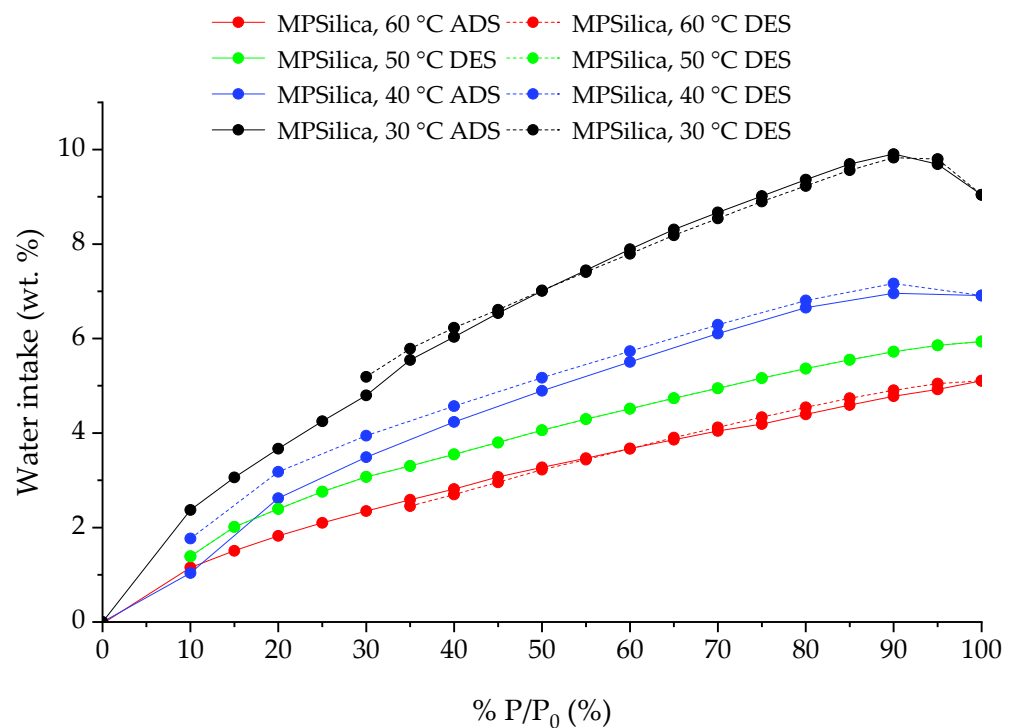


Figure 9. Adsorption and desorption isotherms for MPSilica samples, at 30, 40, 50 and 60 °C.

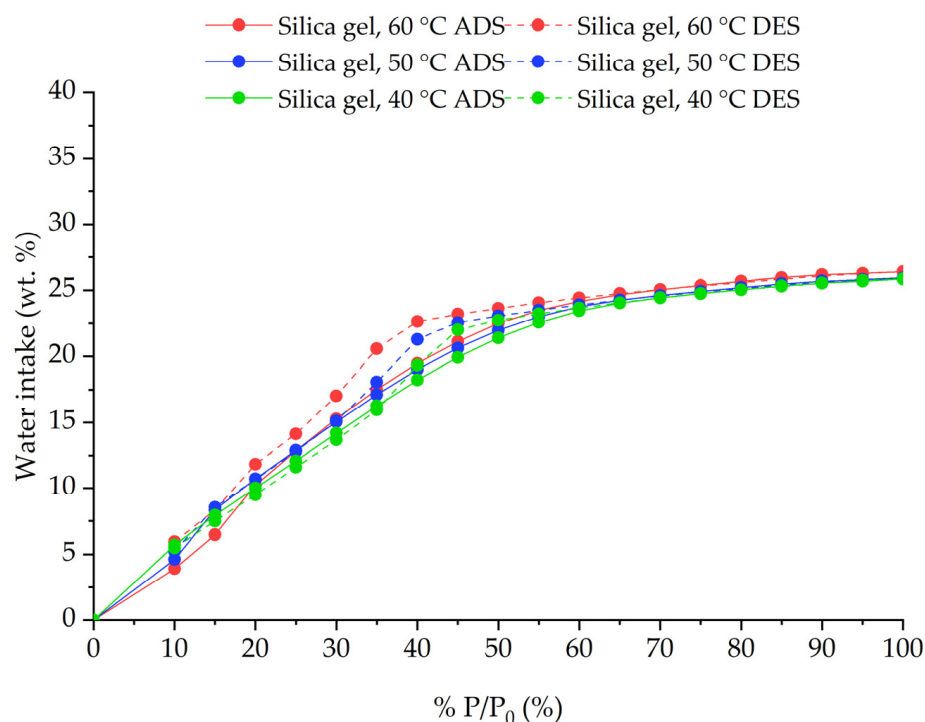


Figure 10. Adsorption and desorption isotherms for Silica gel samples, at 40, 50 and 60 °C.

The AFSMo-Cu sample was characterised by a high increase in mass in relation to the other tested sorbents. The type IV adsorption isotherm with capillary hysteresis characteristic for the H2 type was the highest at the lowest analysed temperature, equal to 30 °C. The results of the BET analysis (presented in Table 2) showed that the specific surface area of this sorbent is not high, as it is less than 300 m²/g, the pore size might be of key importance here, and it was approx. equal to 5 nm. This means that in the case of sorbents dedicated to water adsorption, the pore size (around 5 nm) and the high specific surface area are most important factors.

The highest amount of adsorbed water vapor for the AFSMo-Cu sorbent at 30 °C expressed as the percentage difference between the mass of the reference sample and the mass at a given pressure P/P_0 was 34.93%, while for 40 °C–33.90%, 50 °C–33.92% and 60 °C–33.28%.

The results show that the sorbent can work at low process temperatures, its ability to adsorb water is not dependent on the temperature, but high hysteresis is observed at the lowest process temperature.

The AFSPd-Cu material has a structure similar to the AFSMo-Cu material, it has a much larger specific BET surface area (637 m²/g), but a smaller pore size: approx. 2.5 nm. Therefore, a lower water vapor adsorption capacity of the adsorbent was observed.

Similarly to the previous sorbent, the adsorption isotherm has a type IV shape with a capillary hysteresis of type H2. The highest amount of adsorbed water vapor for the AFSPd-Cu sorbent at 30 °C expressed as a percentage difference between the reference mass of the sample and the mass at a given pressure P/P_0 was 27.39%, while for 40 °C–24.66%, 50 °C–24.81% and 60 °C–25.20%.

Also, in this case, it was observed that the sorbent can work at low process temperatures, its ability to adsorb water is not temperature dependent, and the highest sample mass change was obtained for the lowest process temperature.

The AFSPd-Cu (NP) sorbent is a mixture of AFSPd-Cu and metal nanoparticles (NP). For a P/P_0 of 40%, a characteristic breakdown of the adsorption isotherm was observed, most probably resulting from the presence of nanoparticles in the sample. Metal nanoparticles take the shape of the adsorption isotherm characteristic for type VI, while the AFSPd-Cu sorbent for type II, together, it can be assumed that the shape of the adsorption isotherm

for the AFSPd-Cu (NP) mixture is similar to type III—very rarely present and characteristic for microporous adsorbents.

The highest amount of adsorbed water vapor for the AFSPd-Cu sorbent at 30 °C expressed as water intake at a given pressure P/P_0 was 11.91%, while for 40 °C—10.56%, 50 °C—11.41% and 60 °C—13.12%.

The tested sorbent showed poor water adsorption capacity, which resulted from the low active BET surface area, equal to 52 m²/g.

MP Silica material was characterised by an adsorption isotherm of type I and there was practically no hysteresis, which confirms that the tested material has a microporous structure. The material was characterised by a low water adsorption capacity, although this capacity increased with the temperature decrease. The highest weight gain was observed for the process temperature of 30 °C, for the P/P_0 value of 90% and it was equal to 9.83%. For a temperature of 40 °C, the maximum for P/P_0 90% was 7.16%. On the other hand, for temperatures of 50 and 60 °C, the highest weight gain was observed for P/P_0 equal to 100% and they were 5.94% and 5.11%, respectively.

Despite the large active surface, as the BET surface area was over 2000 m²/g, the material has a microporous structure and the pore size slightly exceeds 2.5 nm, which most likely significantly reduces its ability to adsorb water.

Based on the test results for narrow porous silica gel, it can be concluded that the adsorption isotherms for the temperatures of 40 °C, 50 °C and 60 °C at a water vapor saturation pressure from 10% to 100% P/P_0 according to the IUPAC classification take the shape characteristic for type IV isotherm. Both the shape of the adsorption isotherms and the maximum weight gain of the sorbent are similar in the range of the tested temperatures and equals to a maximum value of 26% on average. In the case of the desorption process, a slight hysteresis is observed, depending on the process temperature and it is characteristic for the type IV isotherm. The hysteresis takes a shape similar to the H2 type, which may indicate that spherical pores with numerous constrictions and open ends are present in the material.

The obtained water adsorption capacities results for analysed materials were compared with literature data and presented in Table 3.

The results of water adsorption for silica gel analysed in this study are slightly lower than in case of literature data, the reason might be a narrow porous structure of the analysed adsorbent. The sorption properties of analysed MOS materials are comparable to those achieved for zeolites, but they are definitely lower than in case of metal organic frameworks (MOFs). As the sorption properties are not the only parameter taken into consideration, but also economic factor is essential, it should be emphasised that the price of silica gels depends upon its purity and structure and in general it is less than 10 €/kg of adsorbent, whereas MOFs prices range is very wide, but starts at about 100 €/g of material. Further modifications of MOS materials might result in their enhanced water adsorption capacity and its value on adsorbent market will definitely increase.

3.5. Simultaneous Thermal Analysis

MOS and a highly porous sample of the silica-based material together with reference sample were tested up to a maximum temperature of 300 °C due to a lack of knowledge about the behaviour of the samples at higher temperatures. The results of thermal analysis are presented in Figure 11.

Table 3. Comparison of water adsorption capacities determined for sorbents analysed in this study with literature data regarding porous materials characterised by high water adsorption capacities.

No.	Material	Process Temperature	Maximal Water Loading, %	Reference
1	AFSMo-Cu	30 °C	35.01	Exp.
2	AFSMo-Cu	40 °C	33.90	Exp.
3	AFSMo-Cu	50 °C	33.92	Exp.
4	AFSMo-Cu	60 °C	33.28	Exp.
5	AFSPd-Cu	30 °C	27.39	Exp.
6	AFSPd-Cu	40 °C	24.66	Exp.
7	AFSPd-Cu	50 °C	24.81	Exp.
8	AFSPd-Cu	60 °C	25.20	Exp.
9	AFSPd-Cu (NP)	30 °C	11.91	Exp.
10	AFSPd-Cu (NP)	40 °C	10.56	Exp.
11	AFSPd-Cu (NP)	50 °C	11.41	Exp.
12	AFSPd-Cu (NP)	60 °C	13.12	Exp.
13	MPSilica	30 °C	9.83	Exp.
14	MPSilica	40 °C	7.16	Exp.
15	MPSilica	50 °C	5.93	Exp.
16	MPSilica	60 °C	5.11	Exp.
17	Silica gel	40 °C	26.39	Exp.
18	Silica gel	50 °C	25.94	Exp.
19	Silica gel	60 °C	25.86	Exp.
20	Silica gel	40 °C	30	[27]
21	TAPSO-34	40 °C	28	[27]
22	Silica gel	25 °C	34.35	[2]
23	Silica gel	40 °C	34.21	[2]
24	Silica gel	60 °C	33.79	[2]
25	MIL-100(Fe)	25 °C	90	[28]
26	MIL-100(Al)	25 °C	50	[28]
27	MOF-841	25 °C	64	[29]
28	MOF-806	25 °C	26	[29]
29	Zeolite 13X	25 °C	33	[29]
30	Zeolites	-	11–38.7	[30]
31	SMOF	-	42	[24]

AFSMo-Cu and AFSPd-Cu samples initially contained high amounts of moisture, which came from the storage of the samples. In both cases below 100 °C, a very fast evaporation of moisture from the surface of the material was observed. The samples were stable in the analysed temperatures range (up to 300 °C), however, a change in their colour was observed after the analysis, which may indicate that some changes in the structure or chemistry may have taken place under the influence of temperature. The sample with the addition of AFSPd-Cu metal nanoparticles showed much longer moisture release, practically, up to 300 °C a change in mass was observed.

For MP Silica sample, a significant loss was observed in the entire analysed temperature range. Almost half of the sample was evaporated up to the temperature of 300 °C, a major thermal decomposition process took place already at 150 °C. Silica gel sample water release was observed in a wider temperature range between 100–200 °C what might affect the kinetics of the adsorption process and the length of the cycle in an adsorption chiller.

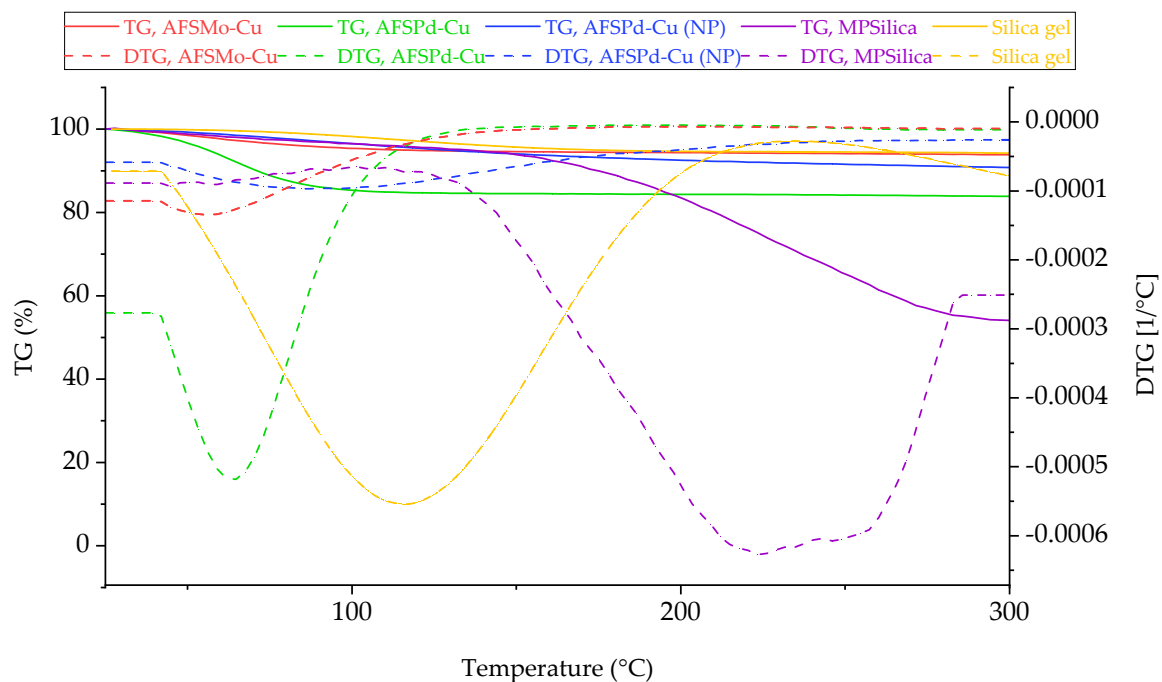


Figure 11. Thermal behaviour of analysed sorbents up to 300 °C in oxidising atmosphere.

4. Conclusions

In this study, four newly developed sorbents were analysed in terms of both, sorption and thermal properties. A possibility to use them in adsorption cooling device driven by low-temperature heat was analysed, and water intake was measured from 30 up to 60 °C. To sum up, MOS materials tested in this study presented enhanced sorption properties in comparison to narrow-porous silica gel. Further modifications of MOS pore size diameter might further increase water sorption properties of these materials and make them even more competitive on the porous materials market. However, addition of metal nanoparticles to MOS samples does not enhance sorption and thermal properties of the adsorbent.

It was noted that in water sorption processes not only active surface area is important, but also pore size defines the water intake properties of the sorbent. Pore diameters smaller than 5 nm are too narrow for water sorption process. Sample AFSMo-Cu was characterised by the smallest active surface area (283.71 m²/g), but mean pore diameter was 5.21 nm, whereas for AFSPd-Cu, BET surface area was 636.62 m²/g and mean pore diameter only 2.5 nm. Comparing water sorption capacities, it was noted that AFSMo-Cu sorption capacity was 33–35%, but for material with higher active surface area it was only 25–27%. Therefore, for adsorption chillers working with water as adsorbate we are looking for adsorbents of large active surface area, pores of diameter higher than 5 nm and noticeable thermal conductivity coefficient. Further modifications of AFSPd-Cu adsorbent pore size diameter might result in definitely larger sorption capacities of the material.

Supplementary Materials: The following supporting information can be downloaded at <https://www.mdpi.com/article/10.3390/en15010368/s1>, Figure S1: Morphology analysis of AFSMo-Cu, Figure S2: Morphology analysis of AFSPd-Cu, Figure S3: Morphology analysis of AFSPd-Cu (NP) Figure S4: Morphology Analysis of MP Silica, Figure S5: Morphology Analysis of Silica gel.

Author Contributions: Conceptualization, K.S. and A.M.-M.; methodology, A.M.-M., N.H.K., W.K. and K.S.; validation, K.S., W.N. and Ł.M.; formal analysis, K.S.; investigation, A.M.-M. and W.K.; resources, K.S., W.N. and Ł.M.; data curation, A.M.-M.; writing—original draft preparation, A.M.-M. and K.S.; writing—review and editing, K.S.; visualization, A.M.-M.; supervision, W.N. and Ł.M.; project administration, Ł.M., W.N. and K.S.; funding acquisition, Ł.M., W.N. and K.S. All authors have read and agreed to the published version of the manuscript.

Funding: This research was funded by Ministry of Science and Higher Education, Poland, grant AGH no 16.16.210.476 and partly supported by program “Excellence initiative—research university” for the AGH University of Science and Technology.

Conflicts of Interest: The authors declare no conflict of interest.

References

1. Sztékler, K.; Kalawa, W.; Mlonka-Medrała, A.; Nowak, W.; Mika, L.; Krzywanski, J.; Grabowska, K.; Sosnowski, M.; Debniak, M. The effect of adhesive additives on silica gel water sorption properties. *Entropy* **2020**, *22*, 327. [[CrossRef](#)]
2. Sztékler, K.; Kalawa, W.; Mika, L.; Mlonka-Medrała, A.; Sowa, M.; Nowak, W. Effect of additives on the sorption kinetics of a silica gel bed in adsorption chiller. *Energies* **2021**, *14*, 83. [[CrossRef](#)]
3. Khadary, N.H.; Ghanem, M.A.; Merajuddine, M.G.; Bin Manie, F.M. Incorporation of Cu, Fe, Ag, and Au nanoparticles in mercapto-silica (MOS) and their CO₂ adsorption capacities. *J. CO₂ Util.* **2014**, *5*, 17–23. [[CrossRef](#)]
4. Kankala, R.K.; Zhang, H.; Liu, C.G.; Kanubaddi, K.R.; Lee, C.H.; Wang, S.B.; Cui, W.; Santos, H.A.; Lin, K.L.; Chen, A.Z. Metal species—Encapsulated mesoporous silica nanoparticles: Current advancements and latest breakthroughs. *Adv. Funct. Mater.* **2019**, *29*, 1902652. [[CrossRef](#)]
5. García-Fernández, A.; Sancenón, F.; Martínez-Mañez, R. Mesoporous silica nanoparticles for pulmonary drug delivery. *Adv. Drug Deliv. Rev.* **2021**, *177*, 113953. [[CrossRef](#)] [[PubMed](#)]
6. Chen, H.; Wang, W.; Wei, X.; Ding, J.; Yang, J. Experimental and numerical study on water sorption over modified mesoporous silica. *Adsorption* **2015**, *21*, 67–75. [[CrossRef](#)]
7. Sierosławska, A.; Borówka, A.; Rymuszka, A.; Żukociński, G.; Sobczak, K. Mesoporous silica nanoparticles containing copper or silver synthesized with a new metal source: Determination of their structure parameters and cytotoxic and irritating effects. *Toxicol. Appl. Pharmacol.* **2021**, *429*, 115685. [[CrossRef](#)]
8. Sachan, D.; Ramesh, A.; Das, G. Green synthesis of silica nanoparticles from leaf biomass and its application to remove heavy metals from synthetic wastewater: A comparative analysis. *Environ. Nanotechnol. Monit. Manag.* **2021**, *16*, 100467. [[CrossRef](#)]
9. Khadary, N.H.; Ghanem, M.A.; Abdesalam, M.E.; Al-Garadah, M.M. Sequestration of CO₂ using Cu nanoparticles supported on spherical and rod-shape mesoporous silica. *J. Saudi Chem. Soc.* **2018**, *22*, 343–351. [[CrossRef](#)]
10. Salazar Hoyos, L.A.; Faroldi, B.M.; Cornaglia, L.M. A coke-resistant catalyst for the dry reforming of methane based on Ni nanoparticles confined within rice husk-derived mesoporous materials. *Catal. Commun.* **2020**, *135*, 105898. [[CrossRef](#)]
11. Garbarino, G.; Cavattoni, T.; Riani, P.; Busca, G. Support effects in metal catalysis: A study of the behavior of unsupported and silica-supported cobalt catalysts in the hydrogenation of CO₂ at atmospheric pressure. *Catal. Today* **2020**, *345*, 213–219. [[CrossRef](#)]
12. Di Natale, F.; Gargiulo, V.; Alfè, M. Adsorption of heavy metals on silica-supported hydrophilic carbonaceous nanoparticles (SHNPs). *J. Hazard. Mater.* **2020**, *393*, 122374. [[CrossRef](#)] [[PubMed](#)]
13. El Kurdi, R.; Chebl, M.; Sillanpää, M.; El-Rassy, H.; Patra, D. Chitosan oligosaccharide/silica nanoparticles hybrid porous gel for mercury adsorption and detection. *Mater. Today Commun.* **2021**, *28*, 102707. [[CrossRef](#)]
14. Venkatesvaran, H.; Kannan, A.; Mayavan, A.; Dhanabal, A.; Gandhi, S. Metal nanoparticle ornated mesoporous silica: A potential nano-interface for uric acid detection. *Microporous Mesoporous Mater.* **2021**, *324*, 111313. [[CrossRef](#)]
15. Chirra, S.; Siliveri, S.; Gangalla, R.; Goskula, S.; Gujjula, S.R.; Adepu, A.K.; Anumula, R.; Sivasoorian, S.S.; Wang, L.F.; Narayanan, V. Synthesis of new multivalent metal ion functionalized mesoporous silica and studies of their enhanced antimicrobial and cytotoxicity activities. *J. Mater. Chem. B* **2019**, *7*, 7235–7245. [[CrossRef](#)] [[PubMed](#)]
16. Endo, A.; Inagi, Y.; Fujisaki, S.; Yamamoto, T.; Ohmori, T.; Nakaiwa, M. *Synthesis of Metal-Doped Mesoporous Silica by Spray Drying and Their Adsorption Properties of Water Vapor*; Elsevier: Amsterdam, The Netherlands, 2007; Volume 165, ISBN 044452178X.
17. Yanagihara, H.; Yamashita, K.; Endo, A.; Daiguji, H. Adsorption-desorption and transport of water in two-dimensional hexagonal mesoporous silica. *J. Phys. Chem. C* **2013**, *117*, 21795–21802. [[CrossRef](#)]
18. Oh, B.; Jabbari-hichri, A.; Bennici, S.; Auroux, A. Enhancing the heat storage density of silica—Alumina by addition. *Sol. Energy Mater. Sol. Cells* **2015**, *140*, 351–360. [[CrossRef](#)]
19. Hashimoto, K.; Kumagai, N.; Izumiya, K.; Takano, H.; Shinomiya, H.; Sasaki, Y.; Yoshida, T.; Kato, Z. The use of renewable energy in the form of methane via electrolytic hydrogen generation using carbon dioxide as the feedstock. *Appl. Surf. Sci.* **2016**, *388*, 608–615. [[CrossRef](#)]
20. Kulakowska, A.; Pajdak, A.; Krzywanski, J.; Grabowska, K.; Zylka, A.; Sosnowski, M.; Wesolowska, M.; Sztékler, K.; Nowak, W. Effect of metal and carbon nanotube additives on the thermal diffusivity of a silica-gel-based adsorption bed. *Energies* **2020**, *13*, 1391. [[CrossRef](#)]
21. Dammel, F.; Ochterbeck, J.M.; Stephan, P. Thermodynamics. In *Springer Handbook of Mechanical Engineering*; Grote, K., Antonsson, E., Eds.; Springer: Berlin/Heidelberg, Germany, 2009; pp. 223–294.
22. Wang, L.W.; Wang, R.Z.; Oliveira, R.G. A review on adsorption working pairs for refrigeration. *Renew. Sustain. Energy Rev.* **2009**, *13*, 518–534. [[CrossRef](#)]
23. Furtado, A.M.B.; Liu, J.; Wang, Y.; Levan, M.D. Mesoporous silica-metal organic composite: Synthesis, characterization, and ammonia adsorption. *J. Mater. Chem.* **2011**, *21*, 6698–6706. [[CrossRef](#)]

24. Palash, M.L.; Jahan, I.; Rupam, T.H.; Harish, S.; Saha, B.B. Novel technique for improving the water adsorption isotherms of metal-organic frameworks for performance enhancement of adsorption driven chillers. *Inorg. Chim. Acta* **2020**, *501*, 119313. [[CrossRef](#)]
25. Yang, Z.; Cao, L.; Li, J.; Lin, J.; Wang, J. Facile synthesis of Cu-BDC/Poly(*N*-methylol acrylamide) HIPE monoliths via CO₂-in-water emulsion stabilized by metal-organic framework. *Polymer* **2018**, *153*, 17–23. [[CrossRef](#)]
26. Feng, Y.; Hu, H.; Wang, Z.; Du, Y.; Zhong, L.; Zhang, C.; Jiang, Y.; Jia, S.; Cui, J. Three-dimensional ordered magnetic macroporous metal-organic frameworks for enzyme immobilization. *J. Colloid Interface Sci.* **2021**, *590*, 436–445. [[CrossRef](#)]
27. Hinze, M.; Ranft, F.; Drummer, D.; Schwieger, W. Reduction of the heat capacity in low-temperature adsorption chillers using thermally conductive polymers as heat exchangers material. *Energy Convers. Manag.* **2017**, *145*, 378–385. [[CrossRef](#)]
28. Karmakar, A.; Prabakaran, V.; Zhao, D.; Chua, K.J. A review of metal-organic frameworks (MOFs) as energy-efficient desiccants for adsorption driven heat-transformation applications. *Appl. Energy* **2020**, *269*, 115070. [[CrossRef](#)]
29. Furukawa, H.; Gándara, F.; Zhang, Y.B.; Jiang, J.; Queen, W.L.; Hudson, M.R.; Yaghi, O.M. Water adsorption in porous metal-organic frameworks and related materials. *J. Am. Chem. Soc.* **2014**, *136*, 4369–4381. [[CrossRef](#)]
30. Tatlier, M.; Munz, G.; Henninger, S.K. Relation of water adsorption capacities of zeolites with their structural properties. *Microporous Mesoporous Mater.* **2018**, *264*, 70–75. [[CrossRef](#)]